

## Supplementary Materials for

### **Acute kidney injury instigates malignant renal cell carcinoma via CXCR2 in mice with inactivated *Trp53* and *Pten* in proximal tubular kidney epithelial cells**

Xunian Zhou<sup>1\*</sup>, Fei Xiao<sup>1\*</sup>, Hikaru Sugimoto<sup>1</sup>, Bingrui Li<sup>1</sup>, Kathleen M. McAndrews<sup>1,†</sup> and Raghu Kalluri<sup>1,2,3,†</sup>

**Supplementary Table 1 Sequences of sgRNAs targeting *Vhl***

<i>Vhl</i> sgRNA 1	CACCGAACTCGCGCGAGCCCTCTC
<i>Vhl</i> sgRNA 2	CACCGACAAAGGCAGCACGACGCGC
<i>Vhl</i> sgRNA 3	CACCGCCCGGTGGTAAGATCGGGT

**Supplementary Table 2 Sequences for amplification of CRISPR/Cas9 targeted region of *Vhl* in T7E1 assay**

<i>Vhl</i> R	GCGTAGATCCGCACGCA
<i>Vhl</i> F	AGGCTTGGTACAAACCTGAAATC

**Supplementary Table 3 Sequences of primers for Q-PCR**

<i>Vhl</i> F	5'-GTATGGCTCAACTTCGACGG-3'
<i>Vhl</i> R	5'-TTAACCAGAAGCCCATCGTG-3'
<i>Gapdh</i> F	5'-AGGTCGGTGTGAACGGATTTG-3'
<i>Gapdh</i> R	5'-TGTAGACCATGTAGTTGAGGTCA-3'
<i>Cxcl1</i> F	5'- CCGAAGTCATAGCCACACTCAA -3'
<i>Cxcl1</i> R	5'- GCAGTCTGTCTTCTTTCTCCGTTA-3'
<i>Cxcr2</i> F	5'-ATGCCCTCTATTCTGCCAGAT-3'
<i>Cxcr2</i> R	5'-GTGCTCCGGTTGTATAAGATGAC-3'

**Supplementary Figure 1 Representative H&E staining of uninvolved organs. (A)**

Representative H&E staining of lung, intestine, liver and pancreas in WT and GPPY mice. Scale bar, 100  $\mu$ m.

**Supplementary Figure 2 Validation of *Vhl* gene knockout *in vitro*. (A)**

Schematic of lentiviral vector for sgRNA expression. U6 promoter was incorporated into the pLentiCRISPRv2 lentiviral vector which drives the expression of the gRNA scaffold, the EFS promoter encodes the codon-optimized SpCas9 transcript and FLAG tag. The indicated BsmBI sites were applied for the insertion of the target sgRNA sequences. **(B)** Three *Vhl* sgRNA sequences were shown in blue, green and red, respectively. **(C)** MCT cells were transduced with LV/Cas9-Control sgRNA, LV/Cas9-Vhl-sgRNA1, LV/Cas9-Vhl-sgRNA2 and LV/Cas9-Vhl-sgRNA3 separately. Cells without transduction were included as WT. Indel formation efficiency was assessed by T7E1 assay. PCR product sizes: sgVhl1, 267 and 535 bp; sgVhl2, 173 and 629 bp; sgVhl3, 218 and 584 bp; G+C positive control, 217 and 416 bp. **(D)** Relative *Vhl* mRNA levels were determined by Q-PCR. Expression data is presented as  $2^{-\Delta\Delta Ct}$  with vector control sgRNA group normalized to a fold change to 1. Data is shown as mean  $\pm$  SEM, n=5. **(E)** Representative western blot of VHL protein. **(F)** Quantification of relative VHL protein levels normalized by  $\beta$ -actin levels and to vector control sgRNA group. Data is presented as mean  $\pm$  SEM, n=5. One-way ANOVA with Tukey post-hoc analysis was used in the indicated groups. \*\* $P < 0.01$ , \*\*\* $P < 0.001$ . **(G)** Quantification of VHL protein levels relative to vector control sgRNA group. Data is presented as mean  $\pm$  SEM, n=5.

**Supplementary Figure 3 Kidney-specific phenotypes associated with deletion of *Trp53*, *Pten* and *Vhl*.** (A) Representative H&E staining of lung, intestine, liver and pancreas in WT and GPPY mice treated with control sgRNA or *Vhl*-sgRNA. Scale bar, 100  $\mu\text{m}$ ; inset scale, 40  $\mu\text{m}$ . (B) Representative images of H&E staining of inflammation and cyst in the indicated experimental groups. Examples of (I) inflammation (D) dysplasia and (C) cyst were circled. Scale bar, 50  $\mu\text{m}$  (top panel) and 100  $\mu\text{m}$  (bottom panel); inset scale, 40  $\mu\text{m}$ . (C) Representative images of IHC staining for HIF-1 $\alpha$ . (D) Quantification of HIF-1 $\alpha$  positive area/visual field (200X). Data is represented as mean  $\pm$  SEM. Control-sgRNAs group: WT, n=3; GPPY, n=3. *Vhl*-sgRNA group: WT, n=3; GPPY, n=3. sgRNA: injected kidney with sgRNA virus mixture solution. Contralateral: contralateral kidney without sgRNA virus injection. One-way ANOVA with Tukey post-hoc analysis was used. \*\*\* $P < 0.001$ . Scale bar, 100  $\mu\text{m}$ ; inset scale, 40  $\mu\text{m}$ .

**Supplementary Figure 4 Phenotypes associated with ischemic kidney injury in GPPY mice.** (A) Representative IRI and contralateral histological sections of kidney from GPPY mice after IRI injury. Examples of (N) necrosis are circled. IRI: injured kidney with IRI surgery. Contralateral: contralateral kidney without IRI surgery. (B) Quantification of necrotic region in kidney. Data is represented as mean  $\pm$  SEM, n=4. (C) Representative images of IHC staining for Ki67. (D) Quantification of Ki67 positive area/visual field (200X). Data is represented as mean  $\pm$  SEM. WT, n=5; GPPY, n=5. (E) Representative H&E staining of lung, intestine, liver and pancreas in WT and GPPY mice with IRI injury. (F) Representative images of immunohistochemical staining of RCC related markers. (G) Representative images of immunohistochemical staining for CXCL1 in WT and GPPY mice without IRI. (H) Quantification of CXCL1 positive area/visual field (200X). Data is represented as mean  $\pm$  SEM. WT, n=5; GPPY, n=5. The significance of B were determined

by unpaired two-tailed t test with Welch's correction. For **D** and **H**, unpaired two-tailed t test were used. \* $P < 0.05$ , \*\* $P < 0.01$ , n.s. not significant. Scale bar, 100  $\mu\text{m}$ ; inset scale, 40  $\mu\text{m}$ .

**Supplementary Figure 5 Isolation of primary kidney dysplastic cells from GPPY mice. (A)**

Kidney cells isolated from GPPY mice with IRI were sorted based on EpCAM expression, with dysplastic cells staining positive for EpCAM and fibroblasts being EpCAM negative. **(B)** Representative images of primary tumor cells from the injured kidney and contralateral kidney prior to sorting, as well as the isolated EpCAM<sup>+</sup> dysplastic cells. Scale bar, 20  $\mu\text{m}$ . **(C)** Recombination PCR of *Trp53* and *Pten* from sorted dysplastic cells for *Trp53* and *Pten* deletion confirmation. Negative ear DNA and cell DNA were purified DNA isolated from ear tissue and dysplastic cells. *Trp53* WT: 835 bp, *Trp53* Flox: 1003 bp. *Trp53* recombination band: 600 bp. *Ggt1-Cre*: 218 bp. *Pten* WT: 350 bp, *Pten* Flox: 480 bp. *Pten* recombination band: 1000 bp. Red arrow denotes the recombined band. **(D)** Flow cytometry analysis of primary kidney cells and splenocytes stained with CD45. **(E)** Kidney cells without IRI were sorted based on YFP positive and negative populations for the separation of dysplastic cells and fibroblasts, respectively. **(F)** Relative *Cxcr2* mRNA levels in fibroblasts derived from the contralateral kidney of IRI mice and kidney without IRI were determined by Q-PCR. Expression value is normalized to fibroblasts from contralateral kidney and is presented as  $2^{-\Delta\Delta\text{Ct}}$ . Data is presented as mean  $\pm$  SEM, n=3. Unpaired two-tailed t test with Welch's correction was used. \*\* $P < 0.01$ .

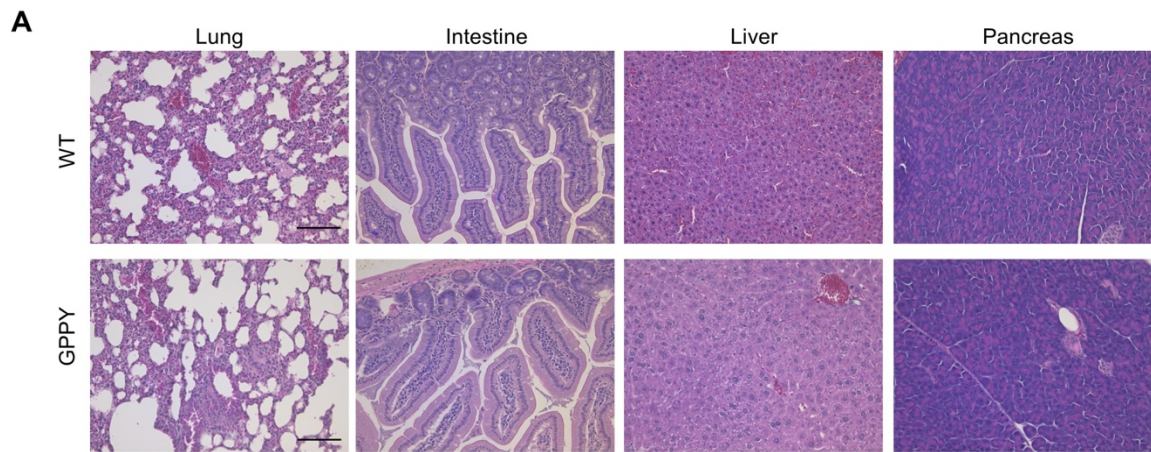
**Supplementary Figure 6 Microenvironment changes in GPPY mice after AKI. (A-D)**

Representative images of IHC staining and quantification for CD68 **(A-B)** and CD163 **(C-D)** from the experimental groups with IRI. Data is represented as mean  $\pm$  SEM. WT, n=5; GPPY, n=5. **(E)**

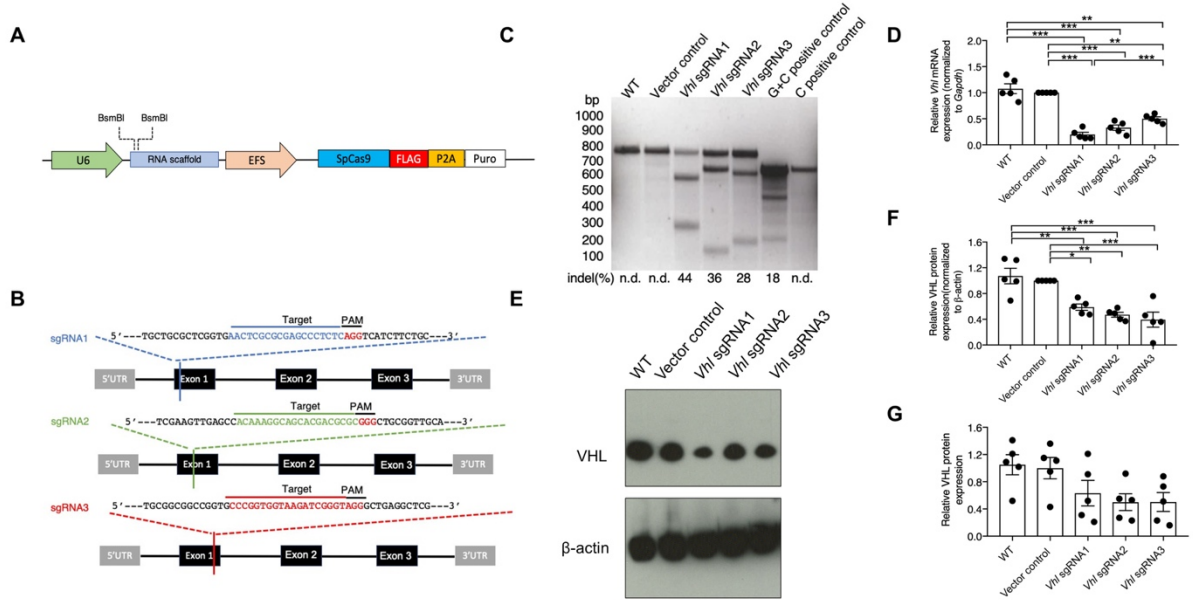
Representative images of co-immunolabeling for CXCR2 (green) with  $\alpha$ SMA (red). **(F)** Quantification of CXCR2 and  $\alpha$ SMA double positive cells/visual field. Data is represented as mean  $\pm$  SEM. WT, n=5; GPPY, n=5. **(G)** Representative images of co-immunolabeling for CXCR2 (green) with vimentin (red). **(H)** Quantification of CXCR2 and vimentin double positive cells/visual field. Data is represented as mean  $\pm$  SEM. WT, n=3; GPPY, n=3. **(I)** Representative images of IHC staining for phospho-p44/42 MAPK (ERK1/2). **(J)** Quantification of phospho-p44/42 MAPK (ERK1/2) positive area/visual field (200X). IRI: injured kidney with IRI surgery. Contralateral: contralateral kidney without IRI surgery. Data is represented as mean  $\pm$  SEM. WT, n=5; GPPY, n=5. For the statistical analysis of **B**, unpaired two-tailed t tests with Welch's correction were used for the comparison of the WT and GPPY groups in IRI and contralateral kidney, unpaired two-tailed t test was used for the comparison of the GPPY groups in IRI and contralateral kidney. One-way ANOVA with Tukey post-hoc analysis was used for the analysis of **D and J**. **\*\* $P < 0.01$ , \*\*\* $P < 0.001$** , Scale bar, 100  $\mu$ m; inset scale, 40  $\mu$ m.

**Supplementary Figure 7 Effects of CXCR2 blockade on distant tissues and stromal cells.** **(A)** Representative H&E staining of lung, intestine, liver and pancreas in WT and GPPY mice with CXCR2 isotype and anti-CXCR2 antibody treatment. **(B-G)** Representative images of immunohistochemical staining and quantification for collagen I **(B-C)**,  $\alpha$ SMA **(D-E)**, CD31 **(F-G)** and CD8 **(H-I)** staining. Data is represented as mean  $\pm$  SEM. CXCR2 isotype treatment group: GPPY, n=5. Anti-CXCR2 antibody treatment group: GPPY, n=5. One-way ANOVA with Tukey post-hoc analysis was used in all the indicated groups. **\* $P < 0.05$ , \*\* $P < 0.01$ , \*\*\* $P < 0.001$** . Scale bar, 100  $\mu$ m; inset scale, 40  $\mu$ m.

**Supplementary Fig.1**

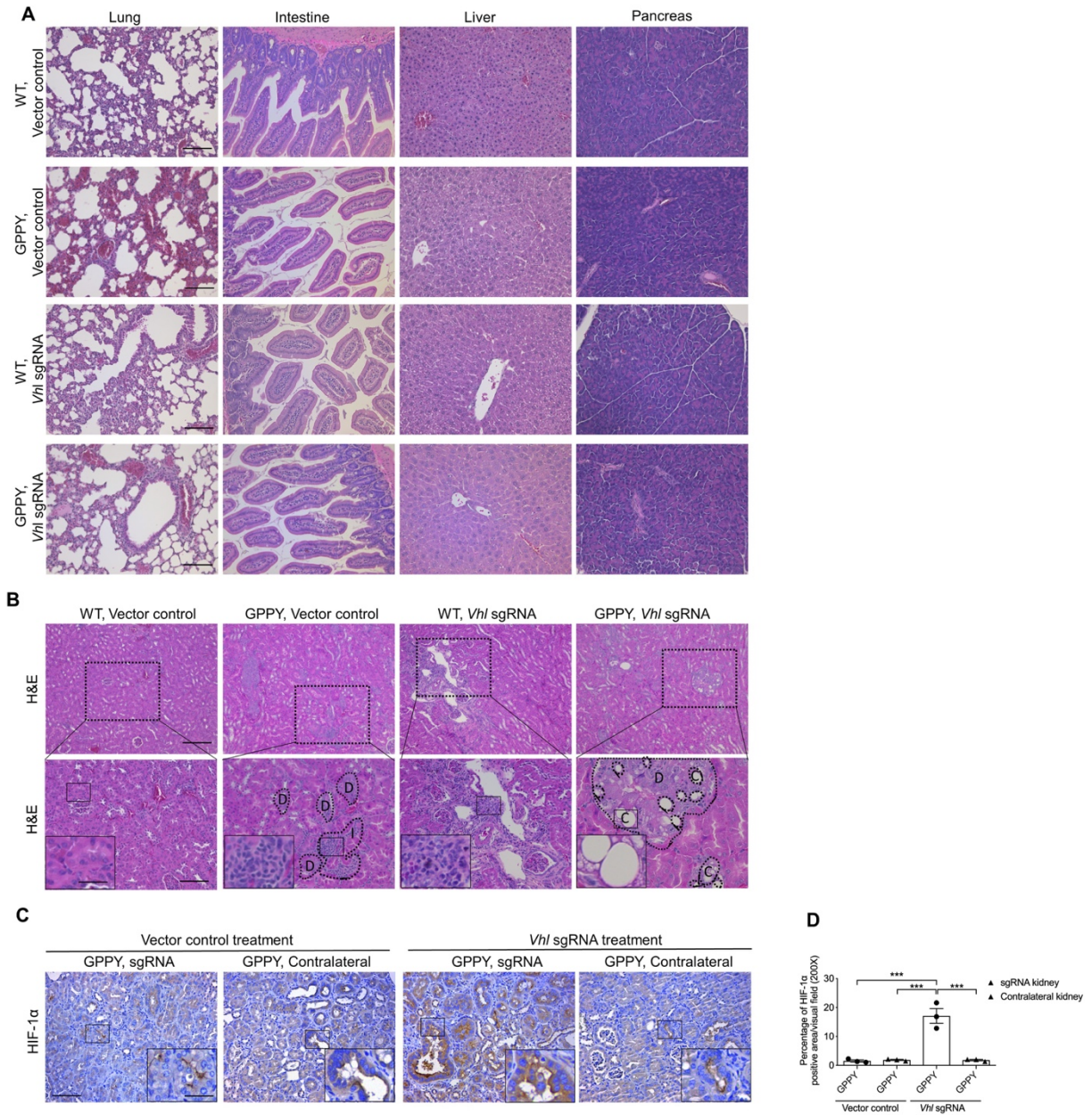


Supplementary Fig.2



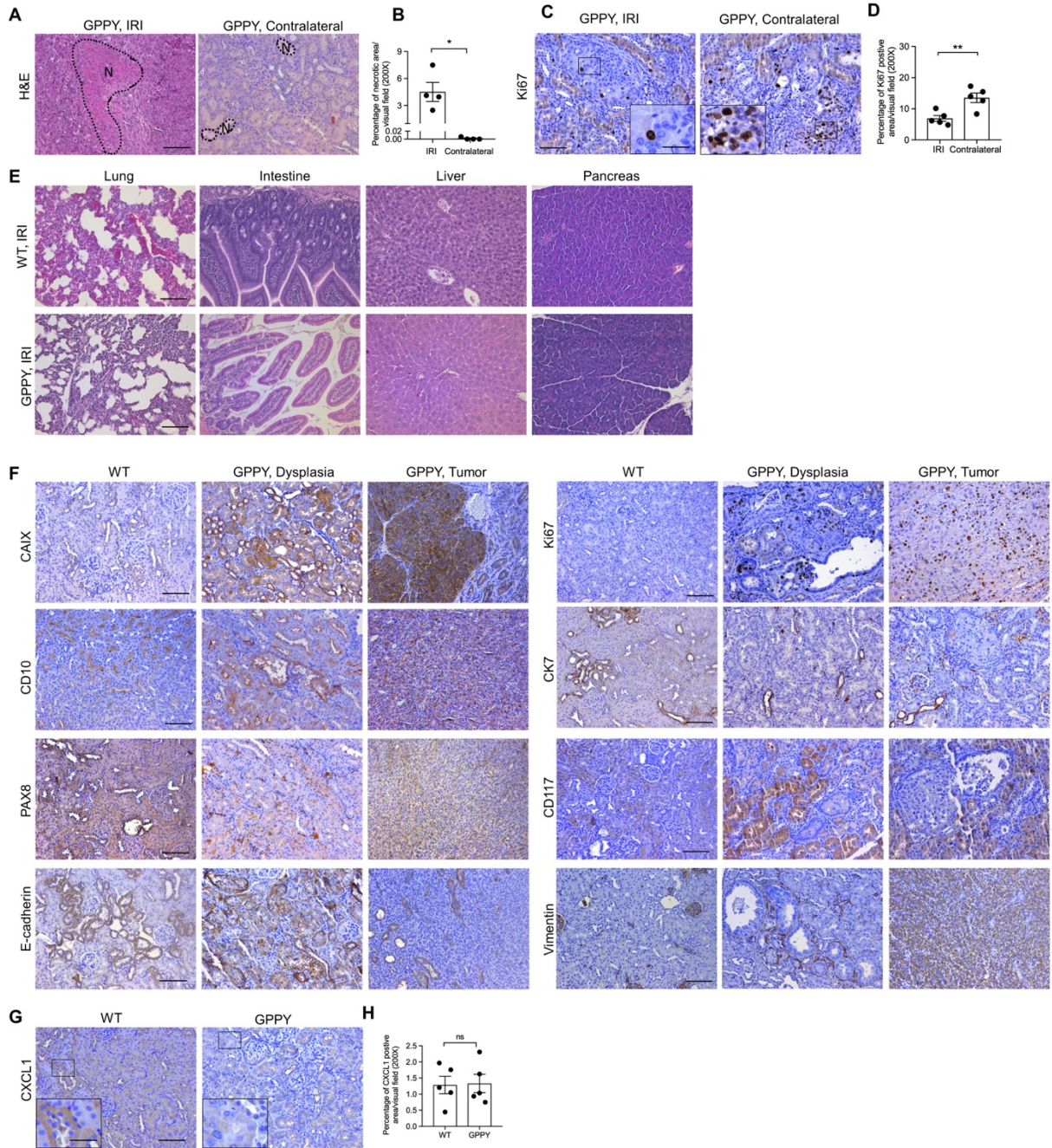


**Supplementary Fig.3**



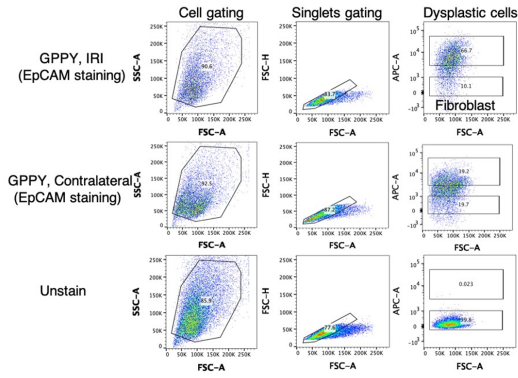


**Supplementary Fig.4**

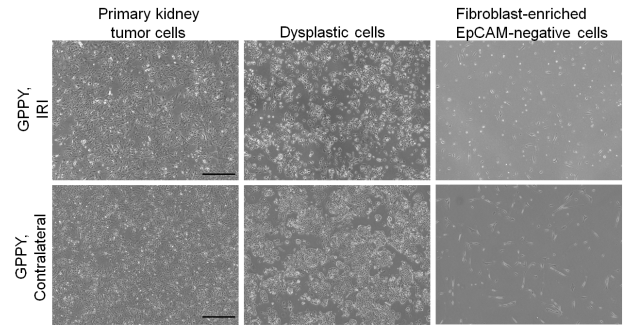


**Supplementary Fig.5**

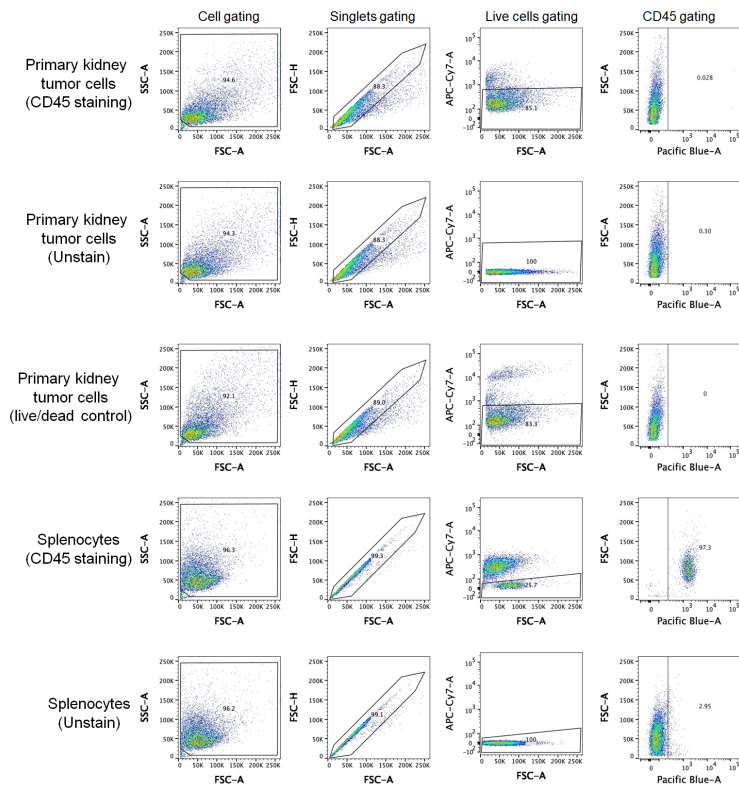
**A**



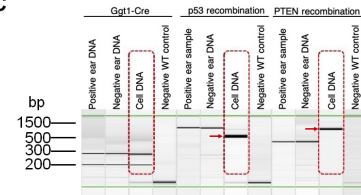
**B**



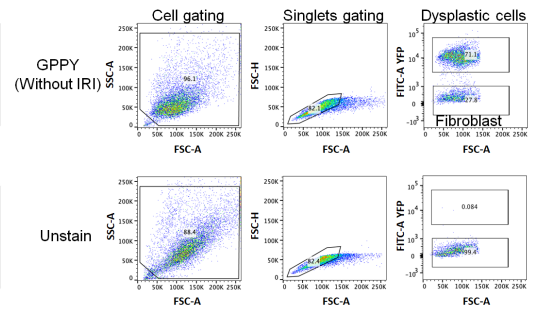
**D**



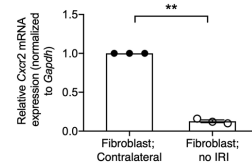
**C**



**E**

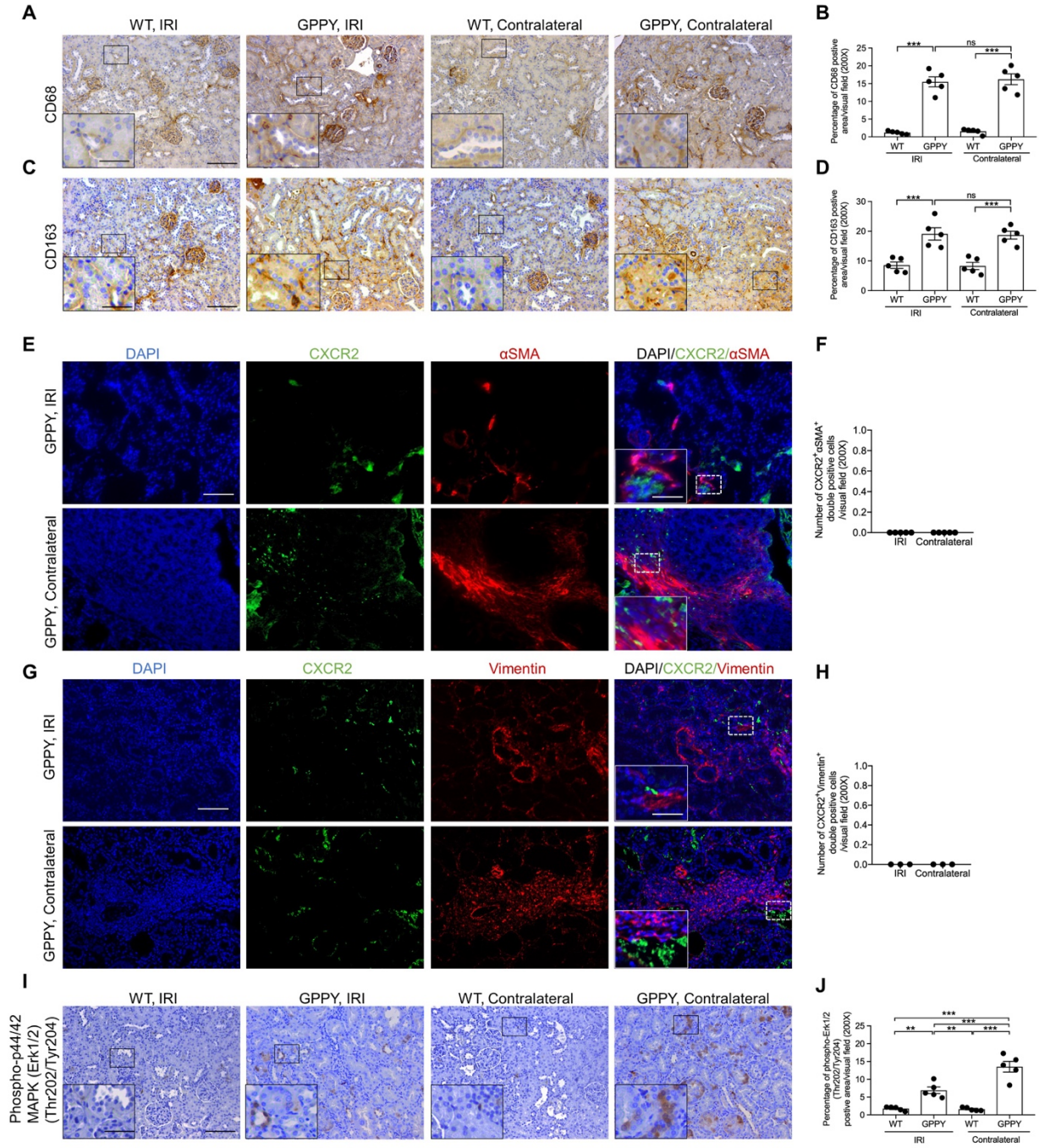


**F**





**Supplementary Fig.6**





**Supplementary Fig.7**

